



Magnetic structure of TbMn_6Ge_6 from neutron diffraction study

G. Venturini^a, B. Chafik El Idrissi^a, E. Ressouche^b, B. Malaman^{a,*}

^aLaboratoire de Chimie du Solide Minéral, Université de Nancy I, Associé au CNRS, URA 158, BP 239, F-54506 Vandoeuvre les Nancy Cedex, France

^bCEA, Département de Recherche Fondamentale sur la Matière Condensée, SPSMS-MDN, 17 Avenue des Martyrs, F-38054 Grenoble Cedex 9, France

Received 22 April 1994

Abstract

Investigations made by susceptibility measurements and neutron diffraction experiments have been performed on the ternary germanide TbMn_6Ge_6 of HfFe_6Ge_6 -type structure ($P6/mmm$). TbMn_6Ge_6 orders ferrimagnetically at $T_c \approx 427$ K but an antiferromagnetic state occurs below about 410 K. Neutron diffraction study shows that both rare earth and manganese sublattices order simultaneously at room temperature. Over the whole 2–300 K temperature range the magnetic structure is a flat spiral consisting of ferromagnetic (001) sheets (with the moments in the layers) of Mn and Tb atoms respectively stacked along the c axis in the sequence Mn1–Tb–Mn2–Mn1–Tb–Mn2. At 2 K, according to the modulation vector $k = (0, 0, \sim 0.125)$, the magnetic moments change their orientation by about 45° within the basal plane on going from one Tb sheet to another, while one observes a spiral turn angle $\theta_1 \approx 31^\circ$ between adjacent Mn1–Tb–Mn2 layers and $\theta_2 \approx 14^\circ$ between Mn2–Mn1 layers, i.e. a repeat distance of about 65 Å. The moment values are $\mu_{\text{Tb}} = 8.43(27) \mu_B$ and $\mu_{\text{Mn}} = 1.84(18) \mu_B$. The magnetic behaviour of TbMn_6Ge_6 is similar to that observed for DyMn_6Ge_6 above 100 K. In the latter case our refinements lead us to propose a new arrangement for the helimagnetic structure previously published, with a Dy magnetic moment corrected to about $9 \mu_B$ at 2 K. The results confirm the interplay between the magnetic coupling and the unit cell volume observed in GdMn_6Ge_6 . A discussion and some comparisons with the parent RMn_6Sn_6 compounds are given in conclusion.

Keywords: Magnetic structure; Neutron diffraction; Susceptibility measurements

1. Introduction

In a previous paper we reported on the crystallographic and magnetic properties of RMn_6Ge_6 ($R = \text{Sc}, \text{Y}, \text{Nd}, \text{Sm}, \text{Gd-Lu}$) compounds [1]. They are isotypic either to HfFe_6Ge_6 [2] ($R = \text{Sc}, \text{Y}, \text{Gd-Lu}$) or to disordered YCo_6Ge_6 [3] ($R = \text{Nd}, \text{Sm}$), both structure types ($P6/mmm$) being built on an alternate stacking of R and T (001) planes in the sequence Mn–T–Mn–Mn–T–Mn. Susceptibility measurements performed between 80 and 800 K have shown that the light rare earth and gadolinium compounds exhibit a spontaneous magnetization whereas the other members of the series are antiferromagnetic (T_N increases from 423 to 509 K between Dy and Lu [1]). In the case of TbMn_6Ge_6 a temperature-dependent metamagnetic-like transition has also been detected below 427 K [1]. Furthermore, neutron diffraction studies clearly indicated that NdMn_6Ge_6 is an easy plane collinear ferromagnet (i.e.

positive Nd–Mn exchange interaction) in the whole temperature range 2–300 K [4]; these studies also confirmed the collinear antiferromagnetic behaviour of YMn_6Ge_6 at room temperature (i.e. diamagnetic rare earth) with an easy axis anisotropic direction [5]. In the latter case it is note worthy that an easy plane occurs in the parent stannide LuMn_6Sn_6 ($T_N = 353$ K) and that both compounds exhibit complex magnetic behaviours at low temperature [5].

More recently Brabers et al. [6] have completed this work by the study of the magnetic properties of several RMn_6Ge_6 compounds ($R = \text{heavy rare earth: Gd-Er}$) and some $\text{R}_{1-x}\text{R}'_x\text{Mn}_6\text{Ge}_6$ solid solutions in the temperature range 2–600 K. They showed that at low temperature the Dy-, Ho- and ErMn_6Ge_6 compounds exhibit a second magnetic transition associated with an antiferromagnetic ordering of both R and Mn sublattices and suggested that T_N marks the onset of antiferromagnetic ordering of the Mn sublattice only. For GdMn_6Ge_6 and to some extent also for TbMn_6Ge_6 , these authors observed magnetic behaviour which can

*Corresponding author.

be described as “bootstrap ferrimagnetism”: at high temperature these compounds clearly behave as typical ferrimagnets, while a bootstrap mechanism related to the unit cell volume variation yields an antiferromagnetic behaviour of both sublattices at low temperature. In contrast with these two germanides, it has been shown that in the parent RMn_6Sn_6 series ($\text{R} \equiv \text{Gd-Ho}$) [7] the ferrimagnetic state remains in the whole ordered temperature range.

Furthermore, during the preparation of this paper, Schobinger-Papamantellos et al. [8] have published their neutron diffraction results on the high and low temperature magnetic structures of DyMn_6Ge_6 . The high temperature magnetic structure is a simple flat spiral consisting of ferromagnetic Dy and Mn layers antiferromagnetically coupled in a three-layer sequence $\text{Mn}(+) - \text{Dy}(-) - \text{Mn}(+)$ (i.e. a unit cell). The moments are in the (001) plane and their directions change by an angle of about 66° on going from one unit cell to another at 300 K (see Fig. 4 of Ref. [8]). Below about 100 K a spin reorientation process occurs on both Dy and Mn sublattices, yielding an incommensurate triple-cone structure along the c axis with a cone angle of about 55° . The two sublattices remain antiferromagnetically coupled over the whole temperature range 300–2 K and lead to net moments $\mu_{\text{Mn}} \approx 2 \mu_{\text{B}}$ and $\mu_{\text{Dy}} \approx 7 \mu_{\text{B}}$ at 2 K.

Because of the numerous magnetic arrangements encountered in both germanide and stannide RMn_6X_6 series, a better understanding of the magnetic interactions in this class of materials clearly requires knowledge of the magnetic structures of all the compounds. In this paper we report on the magnetic structure of TbMn_6Ge_6 determined by neutron diffraction experiments. It will also be shown that our refinements yield a revised description of the helimagnetic component in DyMn_6Ge_6 . All the results will be discussed in the light of those previously obtained for several RMn_6Ge_6 and RMn_6Sn_6 compounds.

2. Experimental procedures

The compounds were prepared from commercially available high purity elements: manganese (powder, 99.9%), terbium (ingot, 99.9%) and germanium (pieces, 99.999%). Pellets of stoichiometric mixture were compacted using a steel die and then introduced into silica tubes sealed under argon (100 mmHg). The samples were annealed for 2 weeks at 1073 K. The purity of the final product was checked by the powder X-ray diffraction technique (Guinier Cu $K\alpha$).

The magnetic measurements were carried out on a Faraday balance (above 300 K) and on a MANICS magnetosusceptometer (between 4.2 and 300 K) in fields up to 1.5 T.

Neutron experiments have been carried out at the Siloe reactor of the Centre D'Etudes Nucléaires de Grenoble (CENG). Several patterns have been recorded in the temperature range 2–300 K with the DN5 multi-detector ($\lambda = 2.4895 \text{ \AA}$).

In the HfFe_6Ge_6 -type structure (space group $P6/mmm$) [2] the Tb and Mn atoms occupy the 1(b): $(0, 0, \frac{1}{2})$ and 6(i): $(\frac{1}{2}, 0, z_{\text{Mn}} \approx \frac{1}{4})$ sites respectively whereas the Ge atoms occupy the 2(c): $(\frac{1}{3}, \frac{2}{3}, 0)$, 2(d): $(\frac{1}{3}, \frac{2}{3}, \frac{1}{2})$ and 2(e): $(0, 0, z_{\text{Ge}} \approx \frac{1}{6})$ sites. Using the scattering lengths $b_{\text{Ge}} = 8.185 \text{ fm}$, $b_{\text{Mn}} = -3.73 \text{ fm}$ and $b_{\text{Tb}} = 7.38 \text{ fm}$ and the form factors of Mn and Tb from Refs. [9] and [10] respectively, the scaling factor, the $z_{\text{Ge, Mn}}$ atomic positions and the Mn and Tb magnetic moments were refined by the mixed crystallographic executive for diffraction (MXD) least-squares-fitting procedure [11]. The MXD program allows simultaneous fitting of the calculated nuclear and magnetic intensities to the observed ones.

3. Experimental results

3.1. Magnetic measurements

Previous investigations have shown that TbMn_6Ge_6 orders at about $T_1 = 427 \text{ K}$ [1]. The thermal variation in the susceptibility in the 4–700 K temperature range ($H_{\text{app.}} = 0.05 \text{ T}$) confirms this value and no further transition occurs down to 4 K. The field dependence of the magnetization at various temperatures is shown in Fig. 1. According to Brabers et al. [6], TbMn_6Ge_6 exhibits a spontaneous magnetization just below the ordering point and becomes antiferromagnetic at a lower temperature ($T < 410 \text{ K}$). Between about 400 and

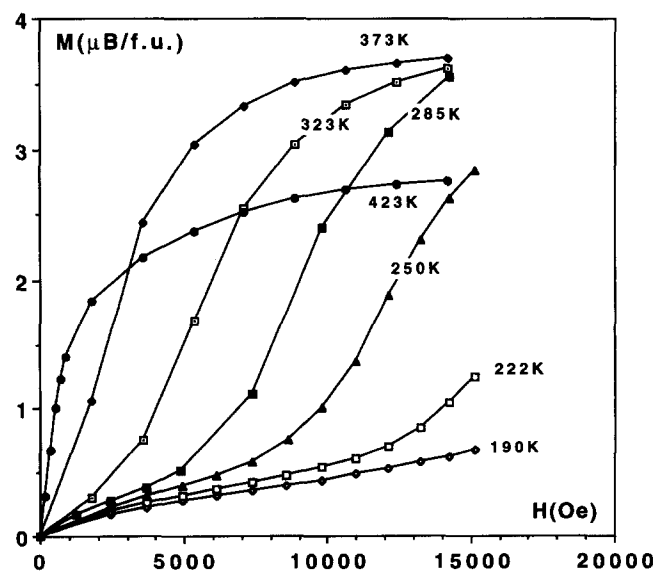


Fig. 1. Field dependence of magnetization at 190, 222, 250, 285, 323, 373 and 423 K in TbMn_6Ge_6 .

190 K a metamagnetic magnetization process occurs, the threshold field increasing with decreasing temperature. Below 190 K the magnetization remains weak and linear with the applied field (up to 1.5 T), indicating that a strong increase in the antiferromagnetic character of both sublattices occurs at low temperature, in agreement with the conclusions of Ref. [6].

3.2. Neutron diffraction study

In agreement with the bulk magnetization measurements, the neutron diffraction patterns recorded step by step from 300 to 2 K (Fig. 2) are identical and display superlattice lines characteristic of an antiferromagnetic ordering. Their Bragg angle values may be indexed as satellites of the nuclear peaks by considering the propagation vector $k=(0, 0, q_z)$ with the q_z value varying from 0.099(1) to 0.125(1) between 300 and 2 K (Fig. 3). Nuclear peaks do not show any magnetic contribution to their intensities, so any commensurate component should be excluded.

The data were fitted to account for a flat spiral arrangement of both Mn and Tb sublattices by refining the magnitude of the moments, their orientation (using the “Euler angle” procedure of the MXD program [11]) and a phase angle relative to each magnetic atom in the unit cell. Bearing in mind the Mn and Tb atomic positions (see Section 2) and assuming that the Mn or Tb moments are ferromagnetically coupled in each (001) layer [5,7], we may distinguish three sets of magnetic atoms (Fig. 4):

- (1) The Mn1 atoms lying in the layer at $z_{\text{Mn1}} \approx \frac{1}{4}$: origin of the phases;
- (2) The Mn2 atoms lying in the layer at $z_{\text{Mn2}} = -z_{\text{Mn1}}$: with a phase angle α_{Mn} ;
- (3) The Tb atoms lying in the layer at $z_{\text{Tb}} = \frac{1}{2}$: with a phase angle α_{Tb} .

Over the whole temperature range studied (300–2 K), the best refinements lead to placing the normal to the spiral plane along the c axis, i.e. the moments are in the (001) plane with a non-zero moment value on both Mn and Tb sublattices (Fig. 4). At 2 K, $\mu_{\text{Mn}} = 1.84(18) \mu_{\text{B}}$ and $\mu_{\text{Tb}} = 8.43(27) \mu_{\text{B}}$ (Table 1); their thermal variations are shown on Fig. 5. Table 1 gives the calculated and observed intensities together with the various adjustable parameters and the lattice constants.

Under these conditions, taking into account the refined phase angles $\alpha_{\text{Mn}} = 8(3)^\circ$ and $\alpha_{\text{Tb}} = 184(10)^\circ$, the Φ angles between the b axis (choose as arbitrary origin of Φ at $z=0$) and the Mn1, Mn2 and Tb moment directions in each successive (001) layer in a unit cell are given by (Fig. 4 and Table 2)

$$\Phi_{\text{Mn1}} = 360q_z z_{\text{Mn1}} \approx 11^\circ$$

$$\Phi_{\text{Mn2}} = 360q_z(1 - z_{\text{Mn1}}) + \alpha_{\text{Mn}} \approx 42^\circ$$

$$\Phi_{\text{Tb}} = 360q_z \frac{1}{2} + \alpha_{\text{Tb}} \approx 206^\circ$$

Therefore the flat spiral magnetic structure consists of ferromagnetic (001) sheets of Mn and Tb atoms respectively stacked along the c axis in the

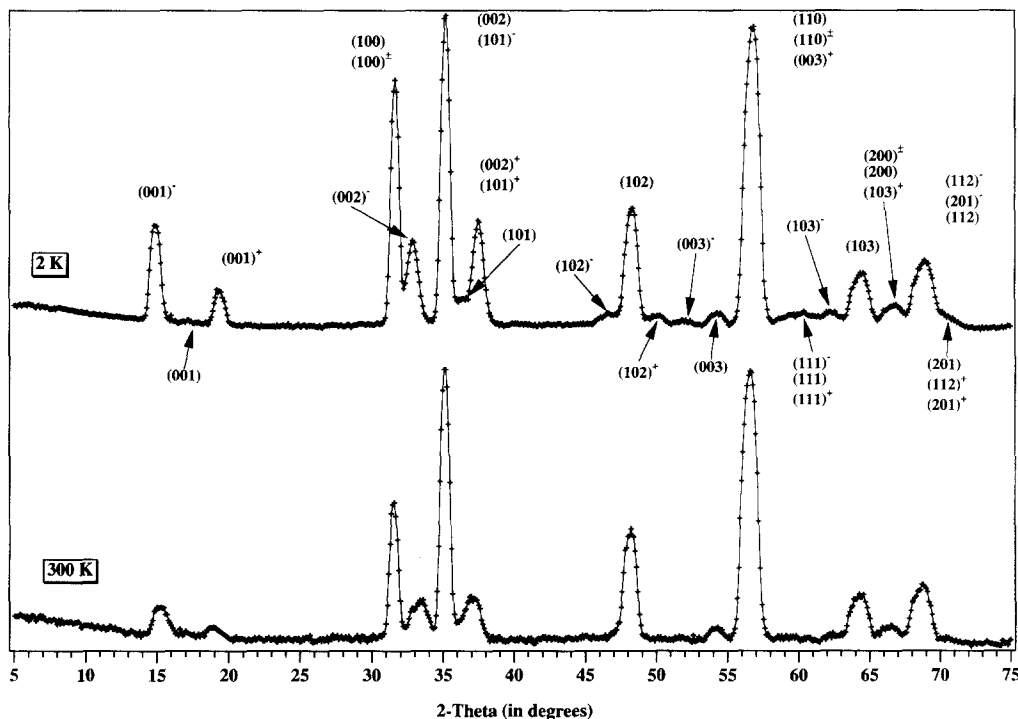


Fig. 2. Neutron diffraction patterns of TbMn_6Ge_6 at 300 and 2 K.

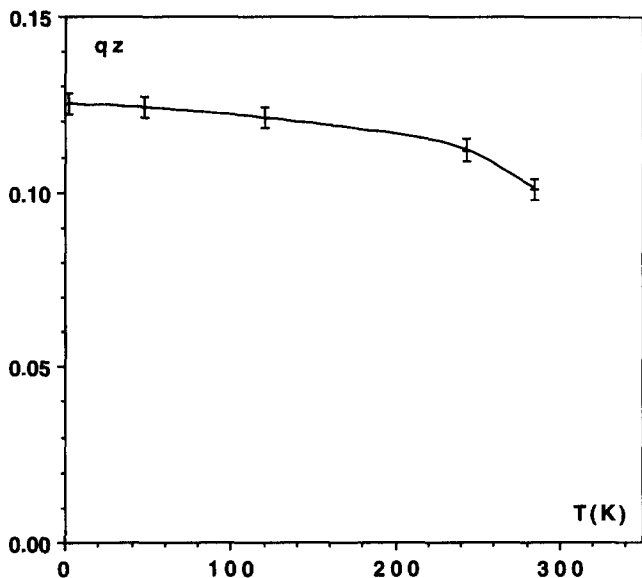


Fig. 3. Temperature dependence of q_z component of wavevector in TbMn_6Ge_6 .

sequence ...Mn1–Tb(Ge)–Mn2–(Ge)–Mn1–Tb(Ge)–Mn2... (Fig. 4). Bearing in mind the q_z component value of the modulation vector (about 0.125), the magnetic moments change their orientation by 45° within the basal plane on going from one Tb sheet to another along the c direction, while one observes a spiral turn angle $\theta_1 \approx 31^\circ$ between adjacent Mn1–Tb(Ge)–Mn2 layers and $\theta_2 \approx 14^\circ$ between Mn2–(Ge)–Mn1 layers (Fig. 4 and Table 2), yielding a repeat distance of about 65 \AA .

Moreover, the angles between the directions of the Tb and Mn moments of adjacent layers (Mn1–Tb(Ge)–Mn2 slabs) are $\theta_3 = 195^\circ$ and $\theta_4 = 165^\circ$ for Mn1–Tb and Mn2–Tb respectively (Fig. 4). Under these conditions the Tb moment direction is antiparallel to the mean direction of the adjacent Mn moments, in agreement with the antiferromagnetic coupling generally observed in heavy rare earth–3d intermetallics, while the Mn moments of the Mn2–(Ge)–Mn1 slabs are almost ferromagnetically coupled (Fig. 4). It is noteworthy that the sign of this latter Mn–Mn exchange interaction is always positive in all known RMn_6X_6 compounds.

3.3. New description of the non-collinear magnetic structure of DyMn_6Ge_6

Since the diffraction patterns of TbMn_6Ge_6 and DyMn_6Ge_6 are strictly similar at room temperature (see Fig. 3 of Ref. [8]), the difference observed between the two magnetic structures appears very surprising. Actually, according to Schobinger-Papamantellos et al. [8], at 293 K the magnetic structure of DyMn_6Ge_6 consists of collinear antiferromagnetic “Mn1–Dy(Ge)–Mn2” slabs (unit cells), the moments collectively chang-

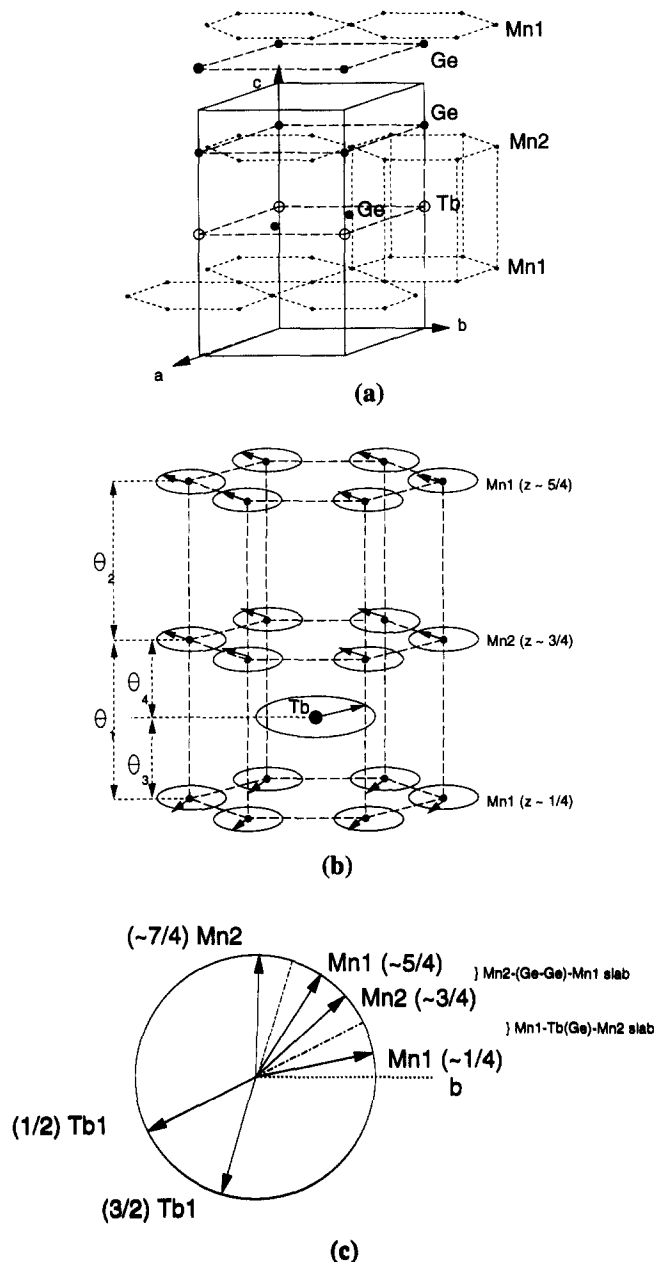


Fig. 4. (a) HfFe_6Ge_6 -type structure. (b) Magnetic structure of TbMn_6Ge_6 . (c) Schematic representation of moment arrangement of flat spiral in $\text{Tb}(\text{Dy})\text{Mn}_6\text{Ge}_6$. The θ_i and various turn angles are given in Table 2.

ing their orientation by 66° within the basal plane on going from slab to slab along the c axis (see Fig. 4 of Ref. [8]). A similar triple-flat-spiral component remains at 2 K with a “turn angle” of 59° . Under these conditions, in contrast with TbMn_6Ge_6 and other RMn_6X_6 compounds, the directions of the Mn moments of the Mn2–(Ge)–Mn1 slabs make angles of about 66° and 58° at 293 and 2 K respectively.

A careful analysis of the published data (Tables 1–3 of Ref. [8]) yields several observations. First, there is a relatively strong misfit between the calculated and observed intensities of the $(001)^+$ and $(001)^-$ satellites,

Table 1
Calculated and observed intensities, lattice constants and adjustable parameters for TbMn₆Ge₆ at 2 K

<i>h k l</i>	<i>I</i> _o	<i>I</i> _c
0 0 1 ⁻	84.4(6)	85.8
0 0 1	2.6(4)	1.4
0 0 1 ⁺	53(1)	57
1 0 0		
1 0 0 [±]	686(3)	641
0 0 2 ⁻	361(3)	357
0 0 2		
1 0 1 ⁻	1182(4)	1197
1 0 1		
1 0 1 ⁺		
0 0 2 ⁺	655(4)	623
1 0 2 ⁻	119(8)	111
1 0 2	1065(8)	1070
1 0 2 ⁺	110(6)	116
0 0 3 ⁻	60(8)	67
0 0 3	227(7)	219
0 0 3 ⁺		
1 1 0		
1 1 0 [±]	4213(11)	4236
1 1 1 ⁻		
1 1 1		
1 1 1 ⁺	358(12)	373
1 0 3 ⁻	239(16)	266
1 0 3	1116(12)	971
1 0 3 ⁺		
2 0 0		
2 0 0 [±]	480(12)	528
1 1 2 ⁻		
1 1 2		
2 0 1 ⁻	1673(17)	1481
2 0 1		
1 1 2 ⁺		
2 0 1 ⁺	186(13)	208
<hr/>		
<i>a</i>	5.205(4) Å	
<i>c</i>	8.144(6) Å	
<i>z</i> _{Ge}	0.162(3)	
<i>z</i> _{Mn}	0.256(3)	
<i>μ</i> _{Mn}	1.84(18) μ _B	
<i>μ</i> _{Tb}	8.43(27) μ _B	
<i>α</i> _{Mn}	8(3)°	
<i>α</i> _{Tb}	184(10)°	
<i>q</i> _r	0.125(1)	
<i>R</i>	4.7%	

with mean reliability factors of about 25% and 31% at 293 and 2 K respectively. Secondly, the observed value of the dysprosium moment is considerably reduced from the theoretical one (7 μ_B against *gJ* = 9 μ_B). The authors have proposed that these discrepancies could originate from the presence of higher order satellites (of the flat spiral component) not detected in the powder data. Bearing in mind these observations, we have re-examined the interpretation of the experiments carried out by Schobinger-Papamantellos et al. [8].

During our refinements we have remarked that a strong correlation occurs between the calculated in-

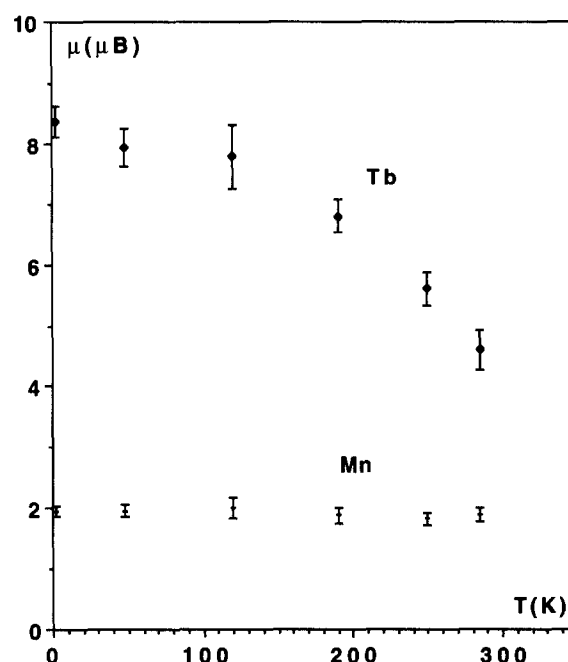


Fig. 5. Temperature dependence of Tb and Mn moment values in TbMn₆Ge₆.

tensities of the (001)⁺ and (001)⁻ satellites and the *α*_{Mn} and *α*_{Tb} phase angle values (see Section 3.2). Using the observed intensities given in Ref. [8], we have refined the phase angles of the flat spiral component and the magnetic moments in DyMn₆Ge₆ with the model defined for TbMn₆Ge₆. At 2 K (where the discrepancies are intensified by the high values of the magnetic moments) our best refinements yield *α*_{Mn} = 10(3)° and *α*_{Dy} = 185(5)° with a mean reliability factor of 4% for the (001)⁺ and (001)⁻ satellites. Similar conclusions hold for the room temperature pattern but with less accuracy. The various *θ*_i, *α*_{Mn, R} and *Φ*_{R, Mn} (see Section 3.2) angles observed in each compound are compared in Table 2. Under these conditions in DyMn₆Ge₆ the Mn-(Ge)-Mn slabs are now nearly ferromagnetically coupled, while in the Mn-Dy-Mn slab the moments deviate by about 20° from collinearity. Lastly, taking into account the ferromagnetic component [8], the resulting moment values are 2.0(1) and 8.9(3) μ_B for Mn and Dy respectively, in fair agreement with the values obtained for the terbium compound.

4. Discussion

The determination of the magnetic structure of TbMn₆Ge₆ yields useful information for a better understanding of its bulk magnetic properties and points out the common features and differences in the magnetic behaviour of the HfFe₆Ge₆-type structure germanides and stannides.

Table 2

Estimated angles in TbMn₆Ge₆ and DyMn₆Ge₆ at room temperature and 2 K (see text and Fig. 4)

	TbMn ₆ Ge ₆		DyMn ₆ Ge ₆	
	2 K	300 K	2 K	293 K
q_z [8]	0.125	0.099	0.163	0.184
Phase angles	$\alpha_{\text{Mn}} = 8(3)^\circ$	$\alpha_{\text{Tb}} = 184(10)^\circ$	$\alpha_{\text{Mn}} = 10(3)^\circ$	$\alpha_{\text{Dy}} = 185(5)^\circ$
“Turn angles” Φ				
Mn1 ($z \approx \frac{1}{4}$)	11°	9°	15°	16.5°
Mn2 ($z \approx \frac{3}{4}$)	42°	35°	54°	60°
Mn1 ($z \approx \frac{5}{4}$)	56°	44.5°	73°	83°
R1 ($z \approx \frac{1}{2}$)	206°	202°	214°	218°
θ_1	31°	26°	39°	43.5°
θ_2	14°	9.5°	19°	23°
$\theta_{3,4}$ (approx.)	165°	167°	161°	158.5°

According to the present neutron study, TbMn₆Ge₆ is a non-collinear antiferromagnet from room temperature to 2 K, in agreement with bulk magnetic measurements. Both Tb and Mn sublattices are ordered till room temperature and this compound exhibits an easy plane as still observed in NdMn₆Ge₆ [4], GdMn₆Ge₆ [12,13] and DyMn₆Ge₆ above 100 K.

The first remark relates to the sign and relative strength of the various R–Mn and Mn–Mn exchange integrals and therefore to the resulting magnetic structure of TbMn₆Ge₆. In this compound the in-plane Mn–Mn and Tb–Tb magnetic interactions are obviously ferromagnetic as observed in all the RT₆X₆ compounds studied. With regard to the tridimensional arrangement, the Tb and Mn sublattices develop a double flat spiral along the *c* axis with turn angle values such that the Mn and Tb moments are nearly antiparallel in an Mn–Tb(Ge)–Mn slab and the Mn moments are almost parallel in an Mn–(Ge)–Mn slab (Fig. 4).

First let us consider the magnetic structure of YMn₆Ge₆ (i.e. Mn sublattice alone). It displays the following dominant Mn–Mn interlayer interactions: the superexchange Mn–Y(Ge)–Mn interactions are antiferromagnetic while, as observed in all the known RMn₆X₆ compounds [4,5,7], the Mn–(Ge–Ge)–Mn interactions are ferromagnetic (see Fig. 5 of Ref. [5]). On the other hand, in the paramagnetic rare earth compounds it is note worthy that the R–Mn couplings are strong enough to return and align the manganese moments of the Mn–R(X)–Mn slabs, giving rise to the ferromagnetic structures of Nd- and SmMn₆Ge₆ [4] and the ferrimagnetic arrangement observed in RMn₆Sn₆ (R ≡ Tb–Er) compounds [7] and GdMn₆Ge₆ at room temperature [6]. Thus one can conclude that in these compounds the Mn–(X)–Mn and R–Mn interactions are dominant.

The analysis of the spin arrangements in TbMn₆Ge₆ and DyMn₆Ge₆ (as described in this work) yields the following observations. The ferromagnetic character of the Mn–(Ge–Ge)–Mn exchange interaction largely re-

mains when the diamagnetic rare earth is replaced by Tb or Dy. A classical negative Tb/Dy–Mn interaction acts mainly in the Mn–R(Ge)–Mn slab, yielding an Mn spin reorientation of about 150° in TbMn₆Ge₆ and about 140° in DyMn₆Ge₆ compared with 180° in the ferro/ferrimagnetic RMn₆X₆ compounds (see above). Obviously, this only partial spin reorientation arises through the competition between negative R–Mn and Mn–Mn interactions in the Mn–R–Mn slab owing to a modification of their relative strengths. Nevertheless, the Tb/Dy–Mn exchange interaction will be relatively strong, since both R and Mn sublattices order at least at room temperature.

As previously proposed by Brabers et al. [6], the magnetic behaviour of these compounds may be explained on the basis of a large increase in the strength of the antiferromagnetic Mn–Mn interactions in the Mn–R(Ge)–Mn slab with a decrease in the Mn–Mn interlayer distances. Under these conditions the occurrence of a ferrimagnetic behaviour at high temperature in TbMn₆Ge₆ has to be related to a dominant negative Tb–Mn exchange interaction. At lower temperature the thermal contraction of the unit cell enhances the antiferromagnetic Mn–Mn interactions of the Mn–Tb(Ge)–Mn slab and the compound becomes helimagnetic. A similar behaviour probably arises in GdMn₆Ge₆, but at lower temperature, owing to the larger room temperature cell parameters and the greater Gd–Mn exchange interactions. Finally, with its smaller unit cell volume and Dy–Mn exchange interaction, the dysprosium compound never exhibits the ferrimagnetic state.

The thermal variation in the wavevector component q_z observed in TbMn₆Ge₆ seems to corroborate this hypothesis, since its value, and therefore the “spin deviation”, decreases as the temperature increases. The q_z value seems to tend to zero at high temperature (Fig. 3), in agreement with the ferrimagnetic behaviour observed closed to T_i in bulk magnetic measurements. In order to check this assumption, a detailed neutron

diffraction study near T_1 is of course highly desirable.

In DyMn_6Ge_6 the q_z value is smaller at 2 K than at room temperature. However, it is note worthy that in this case an additional ferrimagnetic behaviour takes place below 100 K. Therefore in this compound the Mn moment value of the remaining flat spiral component, and correspondingly the strength of the negative Mn–Mn interaction which acts on the Mn–Dy(Ge)–Mn slab, has decreased. It will be very interesting to check this assumption by studying the thermal variation in q_z above 100 K in this compound. Moreover, the correlation which seems to occur between the Mn–Mn interlayer distances and the moment directions in the Mn–R(Ge)–Mn slab in the RMn_6Ge_6 compounds has to be precise and a neutron diffraction study of the magnetic structures of HoMn_6Ge_6 , ErMn_6Ge_6 and TmMn_6Ge_6 appears highly necessary to definitively check this hypothesis. These experiments are in progress.

Finally, one must not forget that, as also noted by Brabers et al. [6], the previously defined correlation between the unit cell volume and the magnetic properties of the RMn_6Ge_6 compounds is not applicable to the corresponding larger RMn_6Sn_6 compounds.

The next remark concerns the easy magnetization direction observed in these compounds. It is note worthy that the change in the easy direction of the manganese moments upon substituting tin by germanium [5] seems also to occur with the rare earths. In LuMn_6Sn_6 the manganese moment lies in the (001) plane. When the anisotropy of the rare earth acts, such as in TbMn_6Sn_6 , a spin reorientation from the basal plane to the c axis occurs [7]. Conversely, in YMn_6Ge_6 the Mn moments are along the c axis, while in the paramagnetic rare earth RMn_6Ge_6 ($R \equiv \text{Nd}$ [4], Gd [6], Tb , Dy) compounds both sublattices exhibit an easy plane. Such a phenomenon has already been discussed in Refs. [5,7], where some explanations can be found.

In another way the occurrence of a ferrimagnetic component, observed below 100 K in DyMn_6Ge_6 , is rather surprising, since the thermal contraction of the cell parameters should enhance the antiferromagnetic behaviour of both sublattices [6]. Under these conditions the low temperature phenomenon might arise because of the rare earth anisotropy, which generally acts mainly in this temperature range.

It is note worthy that in the HoMn_6Sn_6 compound [7] the angle between the moment direction and the c axis is equal to 90° at high temperature, begins to decrease at lower temperature and then locks in an intermediate direction (about 45°). Such behaviour was also observed in the RRh_2X_2 ($X \equiv \text{Si}$, Ge) series, where the terbium compounds exhibit an easy axis while DyRh_2Si_2 and DyRh_2Ge_2 show intermediate moment directions [14]. This deviation of the easy direction from the tetragonal axis was assumed by Takano et al.

to be related to the interplay of the second- and fourth-order crystal electric field coefficients [15]. A similar effect may explain the various easy directions observed in the RMn_6X_6 compounds. The assumption of an interplay between the second- and fourth-order coefficients is corroborated by the weak value of V_{zz} measured in these compounds by Mössbauer spectroscopy [12,16]. Indeed, in DyMn_6Ge_6 such a low temperature variation in the easy direction only yields a reorientation process independently of the exchange interactions previously defined. However, it would imply a drastic effect on the helimagnetic structure, yielding the occurrence of a ferrimagnetic component.

5. Conclusions

The non-collinear antiferromagnetic structure of TbMn_6Ge_6 (and DyMn_6Ge_6) clearly confirms the main influence of the unit cell volume on the magnetic behaviour of the RT_6Ge_6 compounds. The magnetic arrangement arises from the competition between the magnetic contributions from the transition metal and rare earth sublattices. The relative strength of the negative Mn–Mn exchange interactions (in comparison with the R–Mn ones) appears to be strongly correlated to the interatomic interlayer distances. In order to check this point more precisely, it will now be interesting to determine the magnetic structures of HoMn_6Ge_6 , ErMn_6Ge_6 , TmMn_6Ge_6 and TbMn_6Ge_6 near T_1 (about 427 K). Neutron diffraction experiments are under way.

References

- [1] G. Venturini, R. Welter and B. Malaman, *J. Alloys Comp.*, 185 (1992) 99.
- [2] R.R. Olenitch, L.G. Akselrud and Ya.P. Yarmoliuk, *Dopov. Akad. Nauk Ukr. RSR, Ser. A*, (2) (1980) 84.
- [3] W. Bucholz and H.U. Schuster, *Z. Anorg. Allg. Chem.*, 482 (1981) 40.
- [4] B. Chafik El Idrissi, G. Venturini, E. Ressouche and B. Malaman, *J. Alloys Comp.*, 215 (1994) 187.
- [5] G. Venturini, R. Welter and B. Malaman, *J. Alloys Comp.*, 200 (1993) 51.
- [6] J.H.V.J. Brabers, W.H.M. Duijn, F.R. de Boer and K.H.J. Buschow, *J. Alloys Comp.*, 198 (1993) 127.
- [7] B. Chafik El Idrissi, G. Venturini and B. Malaman, *J. Less-Common Met.*, 175 (1991) 143.
- [8] P. Schobinger-Papamantellos, F.B. Altorfer, J.H.V.J. Brabers, F.R. de Boer and K.H.J. Buschow, *J. Alloys Comp.*, 203 (1993) 243.
- [9] C.G. Shull and Y. Yamada, *J. Phys. Soc. Jpn.*, 22 (1962) 1210.
- [10] C. Stassis, H.W. Deckman, B.N. Harmon, I.P. Desclaux and A.J. Freeman, *Phys. Rev. B*, 15 (1977) 369.

- [11] P. Wolfers, *J. Appl. Crystallogr.*, 23 (1990) 554.
- [12] F.M. Mulder, R.C. Thiel, J.H.V.J. Brabers, F.R. de Boer and K.H.J. Buschow, *J. Alloys Comp.*, 190 (1993) L29.
- [13] J.H.V.J. Brabers, V.H.M. Duijn, F.R. de Boer and K.H.J. Buschow, *J. Alloys Comp.*, 198 (1993) 127.
- [14] G. Venturini, B. Malaman, L. Pontonnier, M. Backmann and D. Fruchart, *Solid State Commun.*, 66(6) (1988) 597.
- [15] Y. Takano, K. Ohhata and K. Sekizawa, *J. Magn. Magn. Mater.*, 7(1–3) (1987) 242.
- [16] M.W. Dirken, R.C. Thiel, J.H.V.J. Brabers, F.R. de Boer and K.H.J. Buschow, *J. Alloys Comp.*, 177 (1991) L11.